THE INFLUENCE OF THE LASER IRRADIANCE ON LASER-INDUCED SHOCK WAVES ON MARS

F. Seel[1,2], S. Schröder[1], B. Chide[3], E. Dietz[1], H.-W. Hübers[1,2], [1]German Aerospace Center (DLR), Institute for Optical Sensor Systems, Berlin, Germany; fabian.seel@dlr.de; [2]Humboldt Universität zu Berlin, Institute of Physics, Berlin, Germany; [3]Space and Planetary Exploration Team, Los Alamos National Laboratory, Los Alamos, NM, USA

Introduction: When NASA's Rover Perseverance landed on Mars in 2021, it brought the first operational microphones working in the audible range to Mars [1]. One of the microphones is part of the SuperCam sensor suite that is designed to investigate the composition of Martian rocks and soil from stand-off distances of several meters. SuperCam's microphone can be operated as a standalone instrument or in conjunction with SuperCam's laser-induced breakdown spectroscopy (LIBS) capability. When a LIBS measurement is performed on Mars, a pulsed laser beam is focused on the sample's surface, where some of the material is vaporized and turned into a plasma. Subsequently, the plasma expands due to its high internal pressure into the low-pressure CO_2-dominated atmosphere while generating a shock wave that travels outwards and can be recorded by microphone. The acoustic signal can potentially be used for normalization of LIBS spectra [2], for inferring the sample's hardness [3], for identification of alteration layers [4], or for atmospheric studies [5].

When analyzing the acoustic signal of LIBS measurements, it is important to understand the influence that external parameters, like the laser irradiance on the target that depends on the sampling distance, have on the acoustic signal.

Here, we present first results from measurements investigating the influence of the laser irradiance on the laser-induced shock wave and the subsequent acoustic signal under simulated Martian atmospheric conditions.

Experimental Setup: To investigate how the laser irradiance affects the shock wave generation, its evolution and the acoustic signal, we use a setup that combines three different analytical methods [6,7]. The setup comprises a plasma imaging system to investigate the expansion dynamics of the emitting plasma, a schlieren imaging system to image the expanding shock wave and a microphone to analyze the acoustic signal at larger distances. A sketch of the setup is shown in Figure 1. All measurements were performed inside a simulation chamber that was filled with Mars analogue gas at 710±20 Pa to simulate Martian atmospheric conditions.

The plasma imaging setup is capable of imaging the laser-induced plasma with high temporal resolution of down to 2 ns by using a gated ICCD camera that is most sensitive between about 300 nm and 900 nm [7]. For the presented data, a gating time of 10 ns was used.

The schlieren imaging setup is used to image the density variations in the ambient gas that are induced by the expanding shock wave. To be able to image the laser-induced shock waves at the low Martian ambient pressure, the system was designed for high sensitivity and high temporal resolution. As a light source for background illumination, a laser diode emitting at 900 nm with a pulse time of about 18 ns is used. The illumination time defines the temporal resolution. To achieve the schlieren system's high sensitivity, the light source is collimated and focused on a 5 µm optical slit and a large focal length of 750 mm is used for the focusing lens [6].

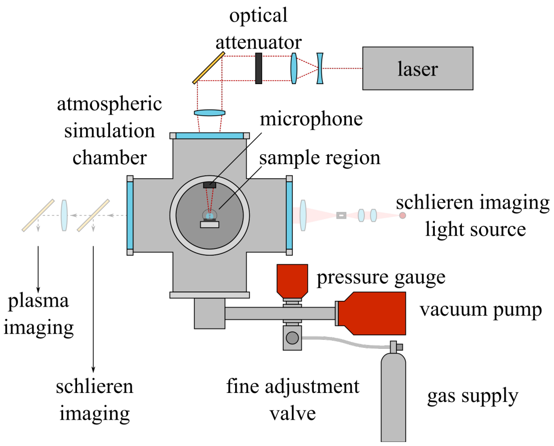

Figure 1: Sketch of the components common to the setup's analytical capabilities. The plasma is induced inside the simulation chamber that can be filled with Martian analogue gas [6].

The microphone used to record the LIBS acoustic signal is mounted inside the simulation chamber at a distance of about 75 mm from the sample surface. Like SuperCam's microphone, it is sensitive to pressure variations between 100 Hz and 10 kHz. It has a sensitivity of about 4.5 mV/Pa.

Methodology: We recorded plasma images, schlieren images and acoustic measurements at different laser energies between about 2 mJ and 19 mJ. By combining the different methods, we cover 5 orders of magnitude in time: The plasma imaging measurements cover the plasma generation and expansion between 0 ns and 2 µs, the schlieren imaging measurements show the shock wave expansion, its decoupling from the plasma plume and the transition to an acoustic wave between 300 ns and 35 µs. The microphone recordings show the pressure signal at larger distances after about 200 µs. Here, we show first results obtained from an iron sample that was chosen due to its homogeneity and strong signals.

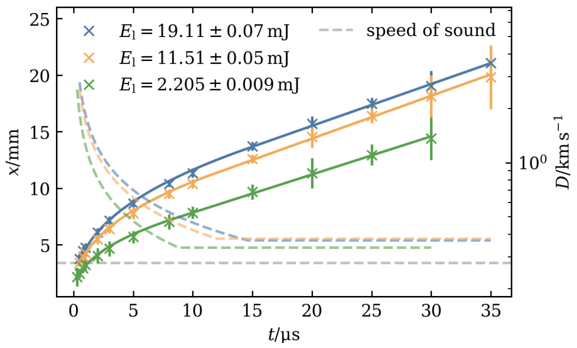

Figure 2: Shock front position x as a function of time after plasma ignition for different laser energies E_l. The first part of the fit function is defined by the Taylor-Sedov model, the second part is a linear function. The derivatives of the fits are shown as dashed lines and refer to the right y-axis.

Results: In Figure 2, the position of the shock front is shown as a function of time after plasma ignition for three different laser energies E_l. With increasing laser energy, the shock wave expansion proceeds faster. The function that is fitted to the data consists of two parts to describe both the supersonic initial expansion phase and also the later phase when the shock wave has already weakened and travels with constant velocity. As seen in previous studies, the first phase is described accurately by the Taylor-Sedov model [6]. After some time t_c, the shock wave has weakened sufficiently that it can no longer be described by the Taylor-Sedov model and now travels with constant velocity. For an acoustic wave moving through an ideal CO_2 atmosphere at room temperature, this velocity would be about $278\,\mathrm{m/s}$. From the secondary y-axis in Figure 2, it can be seen that the slope of the linear part of the fit indicates a velocity D that is faster than the one calculated for the ideal CO_2 gas at room temperature. This could indicate that the ambient atmosphere in the LIBS plasma's vicinity is heated temporarily by the plasma's radiation, which would lead to a faster speed of sound.

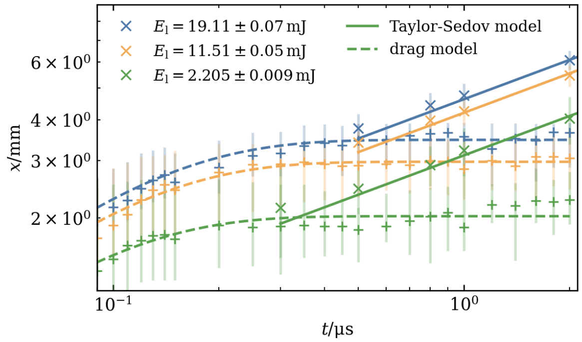

Figure 3: Comparison of the shock front position and the plasma's leading edge position x for different laser energies E_l.

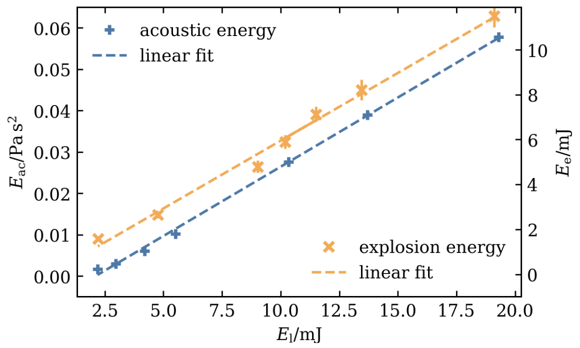

Figure 4: Comparison of the acoustic energy E_{ac} and the explosion energy E_e as a function of laser energy E_l.

In Figure 3, the position of the shock front is compared to the leading position of the emitting plasma at three different laser energies. A drag model is fitted to the plasma front position obtained from the plasma imaging data. After about $300\,\mathrm{ns}$, the plasma stops expanding and its extent remains constant, while the shock wave continues to travel outwards. This marks the decoupling of the shock wave from the plasma front that happens between $300\,\mathrm{ns}$ and $500\,\mathrm{ns}$ after plasma ignition for the different laser energies shown here.

When analyzing LIBS acoustic waves, a commonly used quantity is the acoustic energy E_{ac} calculated from the square of the waveform integrated over the compression phase. In Figure 4, the acoustic energy for different laser energies is compared to the explosion energy E_e that can be computed from the fit of the Taylor-Sedov model in Figure 2. Within the investigated range, the acoustic energy and the explosion energy are correlated and show an approximately linear dependence on the laser energy. However, it should be noted that first results from studies on different materials show a more complex relationship between the acoustic energy and the laser energy.

Conlusion: The presented data give an overview on how changes in the laser irradiance can affect the laser-induced shock wave and the subsequent acoustic signal. We find indications that the plasma might temporarily heat the surrounding atmosphere, leading to an increased speed of sound in the vicinity of the plasma. Furthermore, we show that the shock wave decouples from the plasma between $300\,\mathrm{ns}$ and $500\,\mathrm{ns}$ for different laser energies and that the acoustic energy and the explosion energy of the LIBS shock wave are correlated with the laser energy.

References: [1] Maurice (2021) et al., *Space Sci.*; [2] Lu (2021) et al., *Appl. Phys. B Lasers Opt.*; [3] Chide (2020) et al., *Spectrochim. Acta Part B At. Spectrosc.*; [4] Lanza (2020) et al., *51st LPSC*; [5] Maurice (2022) et al., *Nature*; [6] Seel (2022) et al., *Icarus*; [7] Vogt (2022) et al., *Spectrochim. Acta Part B At. Spectrosc.*